Aerosol single-scattering albedo and asymmetry parameter from MFRSR observations during the ARM Aerosol IOP 2003

E. I. Kassianov, T. P. Ackerman, J. C. Barnard, C. J. Flynn

Atmos. Chem. Phys. Discuss., 6, 13367–13386, 2006
www.atmos-chem-phys-discuss.net/6/13367/2006/

Atmospheric Chemistry and Physics Discussions

Aerosol single-scattering albedo and asymmetry parameter from MFRSR observations during the ARM Aerosol IOP 2003

E. I. Kassianov, T. P. Ackerman, J. C. Barnard, and C. J. Flynn

Pacific Northwest National Laboratory P.O. Box 999 Richland, WA 99352, USA

Received: 30 October 2006 – Accepted: 12 December 2006 – Published: 21 December 2006

Correspondence to: E. Kassianov (debbie.ronfeld@pnl.gov)

Abstract

Multi-filter Rotating Shadowband Radiometers (MFRSRs) provide routine measurements of the aerosol optical depth (τ) at six wavelengths (0.415, 0.5, 0.615, 0.673, 0.870 and 0.94 μm). The single-scattering albedo (ϖ_0) is typically estimated from the MFRSR measurements by assuming the asymmetry parameter (g). In most instances, however, it is not easy to set an appropriate value of g due to its strong temporal and spatial variability. Here, we introduce and validate an updated version of our retrieval technique that allows one to estimate simultaneously ϖ_0 and g for different types of aerosol. We use the aerosol and radiative properties obtained during the Atmospheric Radiation Measurement (ARM) Aerosol Intensive Operational Period (IOP) to validate our retrieval in two ways. First, the MFRSR-retrieved optical properties are compared with those obtained from independent surface, Aerosol Robotic Network (AERONET) and aircraft measurements. The MFRSR-retrieved optical properties are in reasonable agreement with these independent measurements. Second, we perform radiative closure experiments using the MFRSR-retrieved optical properties. The calculated broadband values of the direct and diffuse fluxes are comparable (~5 W/m^2) to those obtained from measurements.

1 Introduction

One of the key uncertainties in the Earth's radiation balance is the effect of aerosols on radiative fluxes, which in turn affects climatic processes on both planetary and local scales (e.g., Hansen et al., 1997; Zhang and Christopher, 2005). Determination of the aerosol-induced radiative flux changes requires information of the aerosol optical properties, such as the aerosol optical depth (τ), single-scattering albedo (ϖ_0) and asymmetry parameter (g) (e.g., Haywood and Shine, 1995; Russell et al., 1997; Andrews et al., 2006). The variation of ϖ_0 can modify not only the magnitude of the aerosol-induced change in top-of-atmosphere upwelling flux, but its sign as well (from a cooling to a heating aerosol effect). The critical value of ϖ_0, where cooling shifts to heating, depends on the surface albedo, τ, and g.

Aerosol properties can be derived through in situ measurements (e.g., Sheridan et al., 2001; Andrews et al., 2004). Commonly, ϖ_0 is estimated from scattering and absorption coefficients measured by an integrating nephelometer and a particle soot absorbance photometer (PSAP), respectively. The asymmetry parameter can be obtained by using measured backscatter fraction (ratio of light scattered into the backward hemisphere to total light scattering) and an appropriate parameterization (e.g., Wiscombe and Grams, 1976). An alternative approach for determining aerosol optical properties is to use combined sun and sky irradiance measurements (e.g., Dubovik et al., 2002; Ricchiazzi et al., 2006). Such measurements are provided by a sunphotometer at four specific wavelengths (0.44, 0.67, 0.87, and 1.02 μm) supported by the Aerosol Robotic Network (AERONET) program (http://aeronet.gsfc.nasa.gov; Holben et al., 1998). This approach allows one to derive aerosol optical properties from size distributions and complex refractive indexes retrieved as part of the AERONET inversion algorithm. Gonzalez-Jorge and Ogren (1996) discussed the uncertainties of aerosol optical properties calculated using aerosol size distributions derived from multiwavelength optical depths.

Widely deployed Multi-filter Rotating Shadowband Radiometers (MFRSRs) measure values of the total and diffuse solar irradiances at six narrowband wavelength channels centered at 0.415, 0.5, 0.615, 0.673, 0.870 and 0.94 μm. These values are used to obtain the direct solar irradiances, which in turn are applied to derive τ (Harrison and Michalsky, 1994; Alexandrov et al., 2002). To estimate ϖ_0, the diffuse to direct ratio (DDR) is commonly used (e.g., Petters et al., 2003; Halthore et al., 2004; Meloni et al., 2005). An iterative process combining measurements of DDR with τ, assumed surface albedo and g is used to retrieve ϖ_0 at a given wavelength. The DDR-derived ϖ_0 values are sensitive to uncertainties/changes of g. For example, Meloni et al. (2005) demonstrated that ± 0.06 variations of g can produce 0.03–0.04 changes of the DDR-derived ϖ_0 at 0.415 μm. Since g is highly variable (Andrews et al., 2006), it is desirable to derive g in addition to τ and ϖ_0 from MFRSR observations.

Previously, we proposed a simple retrieval technique that extends the capability of the MFRSR to study atmospheric aerosols (Kassianov et al., 2005). The technique allows one to estimate the microphysical (e.g., effective radius) and optical (ϖ_0 and g) properties of aerosols. The retrieval is based on measurements of the direct irradiances at two wavelengths (0.415 μm and 0.870 μm) and the diffuse irradiance at 0.415 μm and requires assumptions regarding the shape of the aerosol size distribution (e.g., a combination of three lognormal distributions), the real part of the refractive index, and an estimate of the surface albedo at 0.415 μm. This version works poorly for cases with weak spectral dependence of τ.

In the next section we describe an updated version of this technique, which allows one to perform aerosol retrievals for key types of aerosols (e.g., different loading and spectral dependence of τ) and its further validation using available ground-based and aircraft measurements during the Atmospheric Radiation Measurement (ARM) Program Aerosol Intensive Operational Period (IOP). In Sect. 2 of this paper we review the ARM Aerosol IOP, describe different retrieval techniques, and highlight selected cases. Our MFRSR retrievals of aerosol optical properties are compared with independent retrievals in Sect. 3. Section 4 contains the radiative closure results. In Sect. 5 we present a summary.

2 Approach

The Aerosol IOP ran from 5 May through 31 May 2003, over the ARM Southern Great Plains (SGP) site and yielded numerous case studies spanning a wide range of aerosol situations including well mixed boundary layer cases, as well as cases with distinct elevated aerosol layers (Fig. 1), varying composition, loading and spectral dependence of τ. For example, there are a few elevated aerosol layers for 9 May; according to the aircraft report, one of these layers has high absorption (maybe smoke), another has low absorption (maybe dust). Also, the selected cases are characterized by different aerosol loading. The measured τ for 27 May is close to 0.3 (0.5μm), nearly three times larger than the corresponding τ for 12 May. Also, the Angstrom exponent, which commonly expresses the τ wavelength behavior, changes from 0.69 (9 May) to 1.59 (28 May) (Michalsky et al., 2006). During the Aerosol IOP, the MFRSR observations were accompanied by independent in situ surface and aircraft observations.

Surface measurements of aerosol scattering and absorption coefficients, measured by a three-wavelength nephelometer (0.45, 0.55 and 0.7μm) and one-wavelength PSAP (0.55 μm), are used to derive ϖ_0. These instruments are part of the Aerosol Observing System (AOS) (Sheridan et al., 2001). Commonly, g is derived by using the hemispheric backscatter fraction and an often used parameterization (Wiscombe and Grams, 1976). Andrews et al. (2006) provide a comprehensive overview of available methods for deriving g and their detailed comparisons. To account for the hygroscopic growth of aerosol under ambient humidity conditions, the dry scattering coefficient (at instrumental relative humidity) is adjusted. The CIRPAS Twin Otter aircraft collected data during 15 days, mostly under clear or partly cloudy conditions. As with the surface observations, aircraft measurements of the aerosol scattering and absorption coefficients are measured by nephelometer (0.45, 0.55 and 0.7 μm) and PSAP (0.55 μm) at different altitudes (z). Similar to Andrews et al. (2006), we determine the column-integrated values of g by weighting the individual values of $g(z)$ with measured profiles of the scattering coefficient. We determine the column-integrated values of ϖ_0 by weighting the individual values of $\varpi_0(z)$ with measured profiles of the extinction coefficient.

In order to find comparable datasets (in situ, AERONET and MFRSR) the following two criteria are applied. First, both the aircraft and surface measurements must occur within the same 4-h time period. Since this still allows for a temporal difference between measurements, they may not be coincident in the strict sense. Second, the selected periods must be mostly hemispherically cloud free (hemispherical fractional sky cover ≤0.01). For this selection, we define a "hemispherically cloud free period" as determined by the algorithm of Long and Ackerman (2000). Eight cases are identified

(Table 1). A ground-based CIMEL sun-sky scanning radiometer (part of AERONET) estimates aerosol microphysical and optical properties (e.g., Dubovik et al., 2002). For our comparison we use available cloud-screened data (level 1.5). The CIMEL radiometer was collocated with the AOS, the MFRSR and a normal incidence multifilter radiometer (NIMFR) to within a few hundred meters. Uncertainty of τ can affect substantially the model DDR (e.g., Ricchiazzi et al., 2006) and, thus, the retrieved values of ϖ_0 and g. Michalsky et al. (2006) have shown that bias between the CIMEL-derived and the NIMFR-derived τ values was negligible. To ensure consistency between the CIMEL and MFRSR retrievals of ϖ_0 and g, we simply used τ values obtained from the NIMFR.

The aerosol ϖ_0 and g are derived from MFRSR observations by using an updated version of our retrieval (Kassianov et al., 2005). We create look-up tables to determine parameters of an assumed two-mode size distribution consisting of fine and coarse modes (e.g., Dubovik et al., 2002). In the previous version, the iterative matching procedure varied two parameters of a three-mode size distribution, the total number of particles N and the mean radius R. For each iteration we had to calculate two-dimensional arrays (~50×50 elements) of model aerosol optical depth $\tau_{\text{mod},\lambda}(N,R)$. The new scheme applies look-up tables created for a given two-mode size distribution. Each of the two modes is describing by three parameters for a total of six unknown parameters. The new scheme assumes two parameters (variances of each mode) and estimates the remaining four parameters that represent the integral and the mean particles radius of the fine (N_f,R_f) and coarse (N_c,R_c) modes. Look-up tables substantially speed-up (by a factor of 10) the aerosol retrieval. Replacing two fitting parameters (N and R) by four fitting parameters (N_f, R_f, N_c, R_c) increases the flexibility of the retrieval and its applications. The updated version has been successfully applied to derive optical properties of dust during the major Saharan dust storm of March 2006 (Slingo et al., 2006).

We have also developed a new criterion for matching $\tau_{\text{mod},\lambda}$ and $\tau_{\text{obs},\lambda}$. In the previous version, the iterative matching procedure varied two parameters (N and

ACPD
6, 13367–13386, 2006

EGU

R) until modeled ($\tau_{\text{mod},\lambda}$) and observed ($\tau_{obs,\lambda}$) aerosol optical depths are equal at two wavelengths (0.415 and 0.870 μm). In the updated version, the four parameters (N_f,R_f,N_c,R_c) that produce a minimum of the root-mean square error between $\tau_{\text{mod},\lambda}$ and $\tau_{obs,\lambda}$ at five wavelengths (0.415, 0.5, 0.615, 0.673, 0.870 μm) are considered the best estimate of their true values. This error is defined as a square root of the sum $\frac{1}{k}\sum_{i=1}^{k}\left(\tau_{\text{mod},i}-\tau_{\text{obs},i}\right)^2$, where k is the number of considered wavelengths, equal to 5 here. The determination of four parameters (N_f,R_f,N_c,R_c) is found using an minimization scheme. We expect that the size distribution derived in this manner, while not perfect, will at least be plausible.

Finally, we improve the determination of the imaginary refractive index. Previously, it was estimated from the diffuse irradiance, which depends on the instrument calibration constant, extraterrestrial solar spectrum, stratospheric ozone and nitrogen dioxide. In contrast, the DDR is independent of these factors because the direct and diffuse components are measured by the same sensor and, therefore, these factors are the same for each wavelength irradiance pair, they cancel in the ratio. In our modified version of the retrieval, the imaginary refractive index is estimated from the DDR instead of the diffuse irradiance. Also, the improved version incorporates a circumsolar correction for radiation scattered within the field of view (~3.3 degrees) of the MFRSR. Such a correction can be important for low sun elevation angles, large aerosol loadings and/or large particles sizes.

3 Optical properties

For all MFRSR retrievals we assume that the shape of the aerosol volume size distribution is described by a combination of two lognormal distributions (e.g., Dubovik et al., 2002). This combined distribution has six parameters. We assume that the variances (widths) of fine and coarse modes are equal to 0.5 and 0.7, respectively. Note that the retrieved variances ranged from 0.4 to 0.6 (fine mode) and from 0.6 to 0.8 (coarse mode) for typical aerosols (Dubovik et al., 2002). Other parameters (N_f,R_f,N_c,R_c) are determined during retrieval. To calculate DDR, we apply available spectral values of the surface albedo at five wavelengths (0.415, 0.5, 0.615, 0.673, 0.870 μm) (Michalsky et al., 2006). Also we assume that the real refractive index is equal to 1.5. The MFRSR-retrieved size distribution function and the complex refractive index are used to calculate optical properties of aerosol using Mie theory for each wavelength.

The model and retrieved τ values are in a good agreement (Fig. 2). The good agreement (~1%) is obtained even for the cases with strong vertical variability (9 May and 27 May), low τ (12 May), and relatively weak spectral dependence of τ (9 May). Since in situ measurements provide ϖ_0 and g values at only a single wavelength (0.55 μm), we estimate the AERONET values for this wavelength by using available retrievals at 0.44 μm and 0.673 μm and linear interpolation. To estimate the MFRSR-derived values of ϖ_0 and g at 0.55 μm, a similar interpolation is performed for the MFRSR retrievals at 0.415 μm and 0.67 μm. The MFRSR-retrieved values of ϖ_0 are consistent with independent retrievals (Fig. 3). For example, the relative difference between in situ and MFRSR values is about 3%. Very close agreement between in situ surface and aircraft retrievals may appear surprising especially for cases with strong vertical variability (e.g., 27 May). This variability is most likely associated with the bulk variability in extensive properties such as the extinction coefficient, while intensive aerosol properties (ϖ_0, g) show less variability with altitude.

Figure 4 shows the comparison for the retrieved g values. Similar to ϖ_0, there is good agreement between g values obtained from the in situ surface and aircraft measurements. These values are in the range from 0.55 to 0.65 and represent typical values for dry aerosol (Andrews et al., 2006). The MFRSR-retrieved values of g are larger (0.67±0.03) than those obtained from the in situ retrievals (0.6±0.05). Such differences can reach 12% for a case with low τ (12 May). However, the MFRSR-retrieved g values agree reasonably well with the AERONET retrievals for the majority of cases (Fig. 4) and comparable with the AOS-derived g values (0.65±0.05) obtained at ambient conditions (Andrews et al., 2006).

Sampling issues, temporal difference between measurements (Table 1), and the vertical stratification of aerosol may be responsible for some of the differences between various methods of determining g. It should be mentioned, that none of these methods provide actual determination of the asymmetry parameter. For example, in situ derived values of g (both surface and aircraft) are obtained using measured backscattering fraction and well-known parameterization (Wiscombe and Grams, 1976), while AERONET and MFRSR derived values of g are obtained using the remote sensing instruments (CIMEL and MFRSR), different data inversion techniques, and different samplings. For example, the MFRSR retrieval uses the diffuse irradiance (from hemispherical observations), whereas the AERONET retrieval applies the sky-radiances (from solar almucantar scans during lower sun elevation angles and from the principal plane scans during higher sun elevation angles). In contrast to the AERONET sampling of diffuse radiation (sky scanning), the MFRSR sampling (hemispherical) is independent of the solar zenith angle. Kassianov et al. (2005) discussed differences between the AERONET and MFRSR retrievals. Also, Kassianov et al. (2005) demonstrated that uncertainties in input data (e.g., real refractive index) affect only slightly the MFRSR-retrieved intensive aerosol properties ($\leq$10%) and the diffuse surface irradiances ($\sim$1%). The latter is due to compensation effects of ϖ_0 and g (e.g., overestimation of ϖ_0 is compensated by underestimation of g).

4 Radiative closure

To further validate the MFRSR retrieval, we consider a quantitative comparison that called a closure experiment(e.g., Michalsky et al., 2006; Ricchiazzi et al., 2006). In such an experiment, the measured value of a dependent variable (e.g., the diffuse irradiance) is compared with the value that is calculated from measured/retrieved values of the independent variables (e.g., aerosol optical properties, surface albedo). The outcome of a closure experiment provides a direct evaluation of the combined uncertainty of the radiative transfer (RT) model and measurements/retrievals. Close agreement

ACPD

6, 13367–13386, 2006

between measured and calculated results demonstrates that the RT model and measurements/retrievals may be a suitable representation of the observed system.

Closure experiments have been successfully conducted at the ARM Program's North Slope of Alaska site (Barnard and Powell, 2002) and more recently at the Southern Great Plains (SGP) site (Michalsky et al., 2006). However, prior to these successes obtaining reasonable agreement between model and measured diffuse irradiances at the surface was a long-standing problem; in particular, the model results substantially overestimated the diffuse measurements (e.g., Kato et al., 1997; Halthore et al., 1998). The success of the recent closure experiments (Barnard and Powell, 2002; Michalsky et al., 2006) over a wide range of aerosol cases is attributed to (i) better specification of input parameters (τ, ϖ_0, g, surface albedo) and (ii) more accurate observations of the diffuse irradiance than in previous studies.

Similar to Michalsky et al., (2006), we perform the radiative closure for the direct and diffuse irradiances by using the MFRSR-derived aerosol optical properties and the remaining input parameters (e.g., surface albedo, water vapor). The latter are taken from (Michalsky et al., 2006). Figure 5 shows results of the radiative closure. For both direct and diffuse components, the difference between model calculations and observations is within 5 W/m^2 for the most of the cases. This difference is comparable with measurement uncertainties (Michalsky et al., 2006). The largest difference (~12 W/m^2) is obtained for 27 May (case 5), and a similarly large difference was obtained by Michalsky et al. (2006) for this case. The most likely cause is a small error in the determination of τ. Michalsky et al. (2006) shown that the agreement between the model and measured irradiances can be brought into very good agreement by changing τ by 0.01. This magnitude is the estimated uncertainty of τ derived from well-calibrated measurements (Michalsky et al., 2001). Figure 5 also reveals that, in general, for each case the differences between the model and measured irradiances have similar absolute values for both the direct and diffuse irradiances. The total (direct plus diffuse) fluxes obtained from model calculations and measurements are in very good agreement (~5 W/m^2) in all cases, including case #5.

5 Summary

We have introduced an updated version of our retrieval technique (Kassianov et al., 2005) that uses the MFRSR measurements and makes possible a simultaneous retrieval of the single-scattering albedo (ϖ_0) and the asymmetry parameter (g) from spectral measurements of the direct irradiance and the diffuse to direct ratio (DDR). In comparison with the previous version, the updated version is much faster (by a factor of 10) and more flexible.

Our technique requires assumptions regarding the shape of the aerosol size distribution (two-mode lognormal distributions), the variances (widths) of fine and coarse modes, the real part of the refractive index, as well as the spectral values of surface albedo. The latter can be estimated from satellite or surface measurements. Our technique includes two steps. The first step provides the aerosol size distribution. To do that, we iterate four parameters of two lognormal distributions (integral and mean particles radius of fine and coarse modes) to match the spectral dependence of the aerosol optical depth. The second step estimates the imaginary part of the refractive index for each wavelength. To do that, we iterate values of the imaginary refractive index (for a given size distribution) to match the spectral dependence of the DDR.

We validate our retrieval in two ways. The aerosol and radiative properties obtained during the ARM Aerosol IOP form the basis for this validation. First, the MFRSR-retrieved optical properties are compared with those obtained from independent surface, AERONET, and aircraft measurements. The MFRSR-retrieved values of ϖ_0 are consistent with the other independent retrievals. For example, the relative difference between ϖ_0 obtained from in situ surface measurements and MFRSR values is $\sim$ 5%. For g this difference is within 12% for the case with low τ (12 May). Second, a closure experiment is used to further validate the MFRSR retrieval. Similar to Michalsky et al., (2006), we perform the radiative closure for the direct and diffuse irradiances by using the MFRSR-derived aerosol optical properties and the remaining input parameters (e.g., surface albedo, water vapor) from Michalsky et al. (2006). The calculated broadband values of the direct and diffuse fluxes are comparable (~5 W/m^2) to those obtained from measurements.

The favorable agreement we find between the three types of aerosol retrievals (in situ, AERONET and MFRSR) under a variety of conditions is encouraging and suggests that the updated version of the MFRSR retrieval has the potential for remote sensing of key aerosol types in different locations. Recent successful application of this retrieval to study the dust properties during the major Saharan dust storm of March 2006 (Slingo et al., 2006) supports this expectation.

Acknowledgements. This work was supported by the Office of Biological and Environmental Research of the U.S. Department of Energy as part of the Atmospheric Radiation Measurement (ARM) Program. We thank M. Alexandrov, P. Kiedron, J. Michalsky, J. Ogren, P. Ricchiazzi and D. Turner for providing useful discussions and valuable suggestions.

References

Alexandrov M. D., Lacis, A. A., Carlson, B. E., and Cairns, B.: Remote sensing of atmospheric aerosols and trace gases by means of multifilter rotating shadowband radiometer. Part I: Retrieval algorithm, J. Atmos. Sci., 59, 524–543, 2002.

Andrews, E., Sheridan P., Fiebig, M., McComiskey, A., Ogren, J., Arnott, P., Covert, D., Elleman, R., Gasparini, R., Collins, D., Jonsson, H., Schmid, B., and Wang, J.: Comparison of methods for deriving aerosol asymmetry parameter, J. Geophys. Res., 111, D05S04, doi:10.1029/2004JD005734, 2006.

Andrews, E., Sheridan, P. J., Ogren, J. A., and Ferrare, R.: In situ aerosol profiles over the Southern Great Plains cloud and radiation test bed site: 1. Aerosol optical properties, J. Geophys. Res., 109, D06208, doi:10.1029/2003JD004025, 2004.

Barnard, J. C. and Powell, D. M.: A Comparison Between Modeled and Measured Clear Sky Radiative Shortwave Fluxes in Arctic Environments – With Special Emphasis on Diffuse Radiation, J. Geophys. Res., 107, 4383, doi:10.1029/2001JD001442, 2002.

Dubovik, O., Holben, B., Eck, T. F., Smirnov, A., Kaufman, Y., King, M., Tanre, D., and Slutsker, I.: Variability of absorption and optical properties of key aerosol types observed in worldwide locations, J. Atmos. Sci., 59, 590–608, 2002.

Gonzalez-Jorge, H. G. and Ogren, J. A.: Sensitivity of retrieved aerosol properties to assumptions in the inversion of spectral optical depth, J. Atmos. Sci., 53, 3669–3683, 1996.

Halthore, R., Nemesure, S., Schwartz, S. E., Imre, D. G., Berk, A., Dutton, E. G., and Bergin, M.: Models overestimate diffuse clear-sky irradiance: A case for excess atmospheric absorption, Geophys. Res. Lett., 25, 3591–3594, 1998.

Halthore, R., Miller, M., Orgen, J., Sheridan, P., Slater, D., and Stoffel, T.: Further developments in closure experiments for surface diffuse irradiance under cloud-free skies at a continental site, Geophys. Res. Lett., 31, L07111, doi:10.1029/2003GL019102, 2004.

Hansen, J. E., Sato, M., and Ruedy, R.: Radiative forcing and climate response, J. Geophys. Res., 102, 6831–6864, 1997.

Harrison, L. and Michalsky, J.: Objective algorithms for the retrieval of optical depths from ground-based measurements, J. Appl. Opt., 22, 5126–5132, 1994.

Haywood, J. and Shine, K.: The effect of anthropogenic sulfate and soot aerosol on the clear sky planetary radiation budget, J. Geophys. Res. Lett., 22, 603–606, 1995.

Holben, B., Eck, T. F., Slutsker, I., Tanre, D., Buis, J. P., Setzer, A., Vermote, E., Reagan, J. A., Kaufman, Y. J., Nakajima, T., Lavenu, F., Jankowiak, I., and Smirnov, A.: A federated instrument network and data archive for aerosol characterization, Remote Sens. Environ., 66, 1–16, 1998.

Kassianov, E. I., Barnard, J. C., and Ackerman, T. P.: Retrieval of aerosol microphysical properties by using surface MFRSR data: Modeling and observations, J. Geophys. Res., 110, D09201, doi:10.1029/2004JD005337, 2005.

Kato, S., Ackerman, T. P., Clothiaux, E. E., Mather, J. H., Mace, G. G., Wesely, M. L., Murcray, F., and Michalsky, J.: Uncertainties in modeled and measured clear-sky surface shortwave irradiances, J. Geophys. Res., 102, 25 881–25 898, 1997.

Long, C. N. and Ackerman, T. P.: Identification of clear skies from broadband pyranometer measurements and calculation of downwelling shortwave cloud effects, J. Geophys. Res., 105, 15 609–15 626, 2000.

Meloni, D., di Sarra, A., Pace, G., and Monteleone, F.: Aerosol optical properties at Lampedusa (Central Mediterranean) -2. Determination of single scattering albedo at two wavelengths for different aerosol types, Atmos. Chem. Phys. Discuss., 5, 4971–5005, 2005.

Michalsky, J. J., Schlemmer, J. A., Berkheiser, W. E., Berndt, J. L., Harrison, L. C., Laulainen, N. S., Larson, N. R., and Barnard, J.: Multiyear measurements of aerosol optical depth in the Atmospheric Radiation Measurement and Quantitative Links programs, J. Geophys. Res.,

106, 12 099–12 107, 2001.
Michalsky, J. J., Anderson, G. P., Barnard, J., Delamere, J., Gueymard, C., Kato, S., Kiedron, P., McComiskey, A., and Ricchiazzi, P.: Shortwave radiative closure studies for clear skies during the Atmospheric Radiation Measurement 2003 Aerosol Intensive Observation Period, J. Geophys. Res., 111, D14S90, doi:10.1029/2005JD006341, 2006.
Petters, J. L., Saxena, V. K., Slusser, J. R., Wenny, B. N., and Madronich, S.: Aerosol single scattering albedo retrieved from measurements of surface UV irradiance and a radiative transfer model, J. Geophys. Res., 108(D9), 4288, doi:10.1029/2002JD002360, 2003.
Ricchiazzi, P., Gautier, C., Ogren, J., and Schmid, B.: A comparison of aerosol optical properties obtained from in situ measurements and retrieved from Sun and sky radiance observations during the May 2003 ARM Aerosol Intensive Observational Period, J. Geophys. Res., 111, D05S06, doi:10.1029/2005JD005863, 2006.
Russell, P., Kinne, S., and Bergstrom, R.: Aerosol climate effects: Local radiative forcing and column closure experiments. J. Geophys. Res., 102, 9397–9407, 1997.
Sheridan, P., Delene, D., and Orgen, J.: Four years of continuous surface aerosol measurements from the Department of Energy's Atmospheric Radiation Measurement Program Southern Great Plains Cloud and Radiation Testbed site, J. Geophys. Res., 106, 20 735–20 747, 2001.
Slingo, A, Ackerman, T., Allan, R., Kassianov, E., McFarlane, S., Robinson, G., Barnard, J., Miller, M., Harries, J., Russell, J., and Dewitte, S.: Observations of the impact of a major Saharan dust storm on the Earth's radiation budget, J. Geophys. Res. Lett., in press, 2006.
Wiscombe, W. and Grams, G.: The backscattering fraction in two-stream approximations, J. Atmos. Sci., 33, 2440–2451, 1976.
Zhang, J. and Christopher, S.: Shortwave aerosol radiative forcing over cloud-free oceans from Terra: 2. Seasonal and global distributions, J. Geophys. Res., 110(D10S24), doi:10.1029/2004JD005009, 2005.

Table 1. Day and time (UTC) for surface, AERONET, and aircraft measurements for eight selected cases.

		Time		
Case	Day	Surface	AERONET	Aircraft
1	09 May	17:30	17:28:30	15:28–20:10
2	12 May	15:50	17:28:27	14:48–19:09
3	20 May	20:00	20:28:31	14:49–18:27
4	22 May	14:00	17:28:45	08:25–13:13
5	27 May	19:00	19:29:16	14:20–19:29
6	28 May	24:00	20:29:20	18:24–22:05
7	29 May	14:30	16:29:30	14:11–17:51
8	29 May	18:30	17:29:33	14:11–17:51

ACPD

6, 13367–13386, 2006

Aerosol single-scattering albedo and asymmetry parameter

E. I. Kassianov et al.

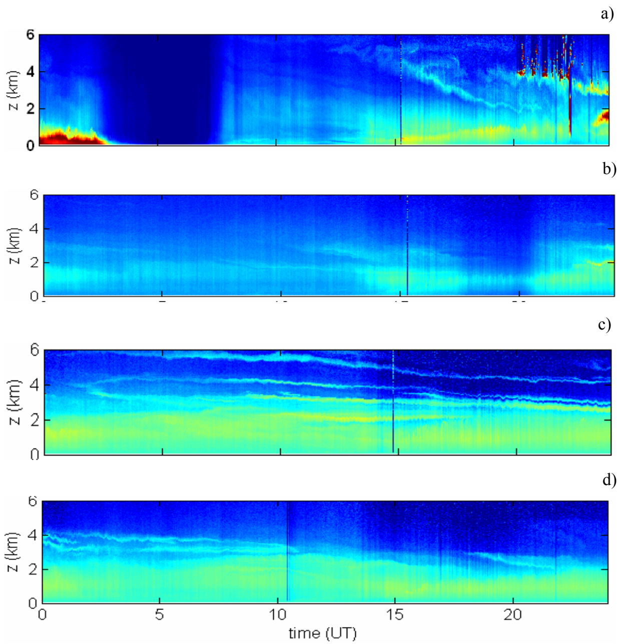

Fig. 1. Two-dimensional images of micropulse lidar backscatter for 9 May **(a)**, 12 May **(b)**, 27 May **(c)**, and 29 May **(d)**; horizontal axis – time (UT), vertical axis – altitude (km). Increasing color wavelength (blue to yellow to red) represents increasing backscatter.

ACPD
6, 13367–13386, 2006

Title Page
Abstract Introduction
Conclusions References
Tables Figures
◀I ▶I
◀ ▶
Back Close
Full Screen / Esc
Printer-friendly Version
Interactive Discussion

EGU

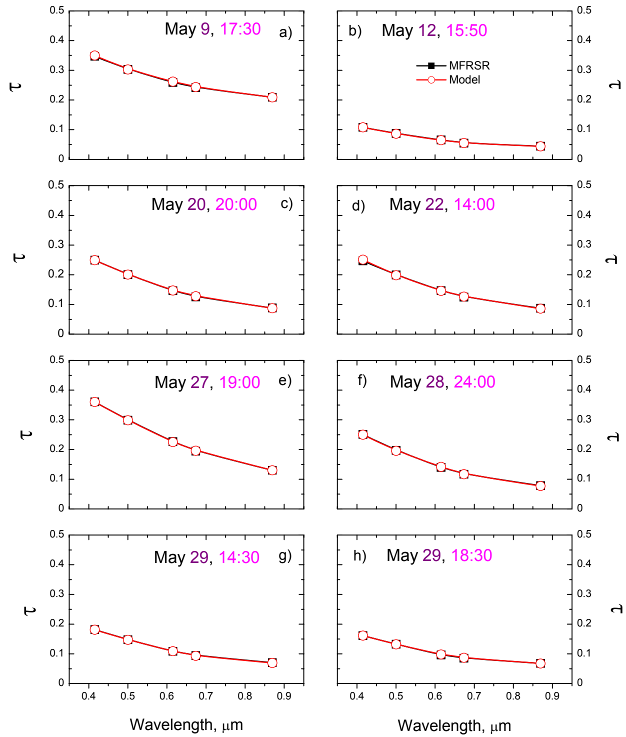

Fig. 2. The spectral dependence of the aerosol optical depth τ for selected cases: τ derived from the MFRSR data (square) and τ obtained from Lorenz-Mie calculations (circle) by using the derived aerosol size distribution and refractive index.

ACPD
6, 13367–13386, 2006

Aerosol single-scattering albedo and asymmetry parameter

E. I. Kassianov et al.

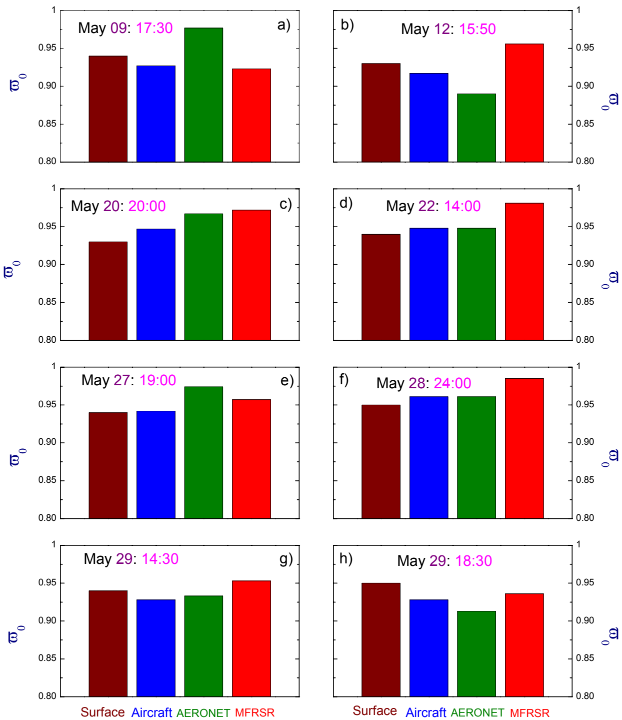

Fig. 3. Single-scattering albedo (ϖ_0) derived from the in situ surface (brown), aircraft (blue), AERONET (green) and MFRSR (red) data at 0.55 μm wavelength.

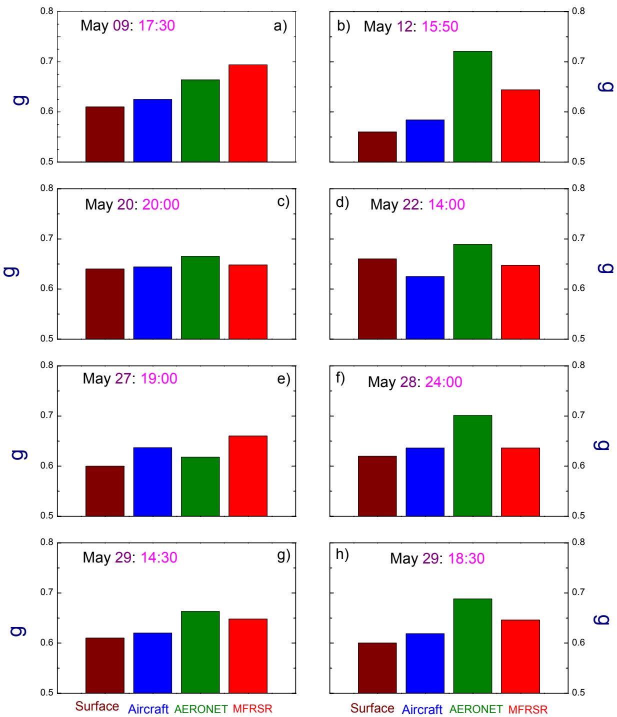

Fig. 4. The asymmetry parameter (g) derived from the in situ surface (brown), aircraft (blue), AERONET (green) and MFRSR (red) data at 0.55 μm wavelength.

ACPD

6, 13367–13386, 2006

Aerosol single-scattering albedo and asymmetry parameter

E. I. Kassianov et al.

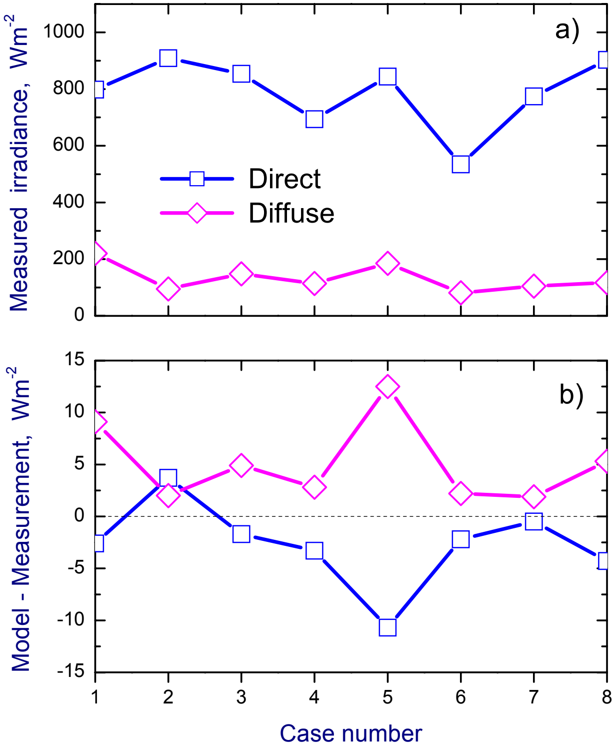

Fig. 5. **(a)** Measured direct and diffuse irradiances and **(b)** the corresponding differences (model-measurements) of direct and diffuse irradiances as function of case number.

ACPD

6, 13367–13386, 2006

Aerosol single-scattering albedo and asymmetry parameter

E. I. Kassianov et al.

EGU